Biophysical Journal Volume 83 December 2002 2969–2980

Structure and Energy of Fusion Stalks: The Role of Membrane Edges

Sylvio May
Institut für Molekularbiologie, Friedrich-Schiller-Universität Jena, 07745 Jena, Germany

ABSTRACT Fusion of lipid bilayers proceeds via a sequence of distinct structural transformations. Its early stage involves a localized, hemifused intermediate in which the proximal but not yet the distal monolayers are connected. Whereas the so-called stalk model most successfully accounts for the properties of the hemifused intermediate, there is still uncertainty about its microscopic structure and energy. We reanalyze fusion stalks using the theory of membrane elasticity. In our calculations, a short (cylindrical micelle-like) tether connects the two proximal monolayers of the hemifused membranes. The shape of the stalk and the length of the tether are calculated such as to minimize the overall free energy and to avoid the formation of voids within the hydrocarbon core. Our free energy expression is based on three internal degrees of freedom of a perturbed lipid layer: thickness, splay, and tilt deformations. Based on exactly the same model, we compare fusion stalks with and without the ability included to form sharp edges at the interfacial region between the hydrocarbon core and the polar environment. Requiring the interface to be smooth everywhere, our detailed calculations recover previous results: the stalk energies are far too high to account for the experimental observation of fusion intermediates. However, if we allow the interface to be nonsmooth, we find a remarkable reduction of the stalk free energy down to more realistic values. The corresponding structure of a nonsmooth stalk exhibits sharp edges at the transition regions between the bilayer and tether parts. In addition to that, a corner is formed at each of the two distal monolayers. We discuss the mechanism how membrane edges reduce the energy of fusion stalks.

INTRODUCTION

Membrane fusion requires transient structural reorganization of at least some lipids (for recent reviews, see Jahn and Südhof, 1999; Lentz et al., 2000; Epand, 2000; Burger, 2000; Chernomordik and Zimmerberg, 1995). Experimental (Chanturiya et al., 1997; Chernomordik et al., 1995a; Zimmerberg et al., 1993) evidence points to the existence of so-called hemifusion structures, which are relatively long-living intermediates appearing during the early stage of fusion. Such intermediate structures are found for fusion events that do or do not involve specialized fusion proteins (Chernomordik et al., 1997), suggesting their generic and lipid-based nature.

Fusion intermediates are likely to set energy barriers that the fusion process has to overcome. Thus, they are essential determinants of the fusion rate. Fusion intermediates may also have played a role for the evolution of the fusion protein machinery (Lee and Lentz, 1997). Yet, until now little structural information is available because experimental methods that probe structural aspects of the highly localized fusion intermediates are rather limited. Therefore, various theoretical models of the fusion scenario have been suggested (Siegel, 1993; Noguchi and Takasu, 2001; Müller et al., 2002). Of particular interest is the formation of an initial, hemifused; intermediate structure in which only the lipids of the proximal monolayers of two fusing bilayers mix. So far, the so-called stalk model (Kozlov and Markin, 1983) is the most consistent hypothesis for the hemifusion intermediate (Gaudin, 2000; Basánez et al., 1997, 1998). The stalk consists of a lipidic tether that connects the two proximal monolayers of the fusing membranes[1], as shown in Fig. 1 *A*. The stalk represents a metastable state. That is, even in its optimal conformation, it entails a positive free energy penalty (compared with an unperturbed lipid bilayer). The magnitude of this energy is important for the rate of the initial fusion events.

In previous models (Siegel, 1993, 1999), the free energy of a fusion stalk was calculated based upon the energy needed to bend the involved lipid monolayers. A second energy contribution has to be included in this kind of models. This so-called interstitial energy accounts for the formation of a void region within the hydrophobic core of a fusion stalk (a similar interstitial energy appears in the inverse-hexagonal, H_{II}, phase). It turned out that particularly due to the interstitial energy the predicted energies of the fusion stalks were too high to account for the experimental observation of hemifusion intermediates. Stalks with energies of considerably more than 100 k_BT (in which k_B is the Boltzmann constant and T the absolute temperature) are very unlikely to serve as the hemifusion intermediate. In fact, Kuzmin et al. (2001) have estimated that the stalk energy should not exceed a value of about 40 k_BT to appear within the experimentally observed time scale. Hence, the apparent energetic discrepancy calls for either an alternative structural model of the fusion stalk or a new concept in calculating its energy.

Very recently, the "energy crisis" was solved by an elegant work of Kozlovsky and Kozlov (2002). They have suggested a modified structural model of the fusion stalk (Fig. 1 *B*) in which the two proximal monolayers of fusing

Submitted January 30, 2002; and accepted for publication August 8, 2002.
Address reprint requests to Sylvio May, Winzerlaer Strasse 10, 07745 Jena, Germany. Tel.: 49–3641-657582; Fax: 49–3641-657520; E-mail: may@lily.molebio.uni-jena.de.

0006-3495/02/12/2969/12 $2.00

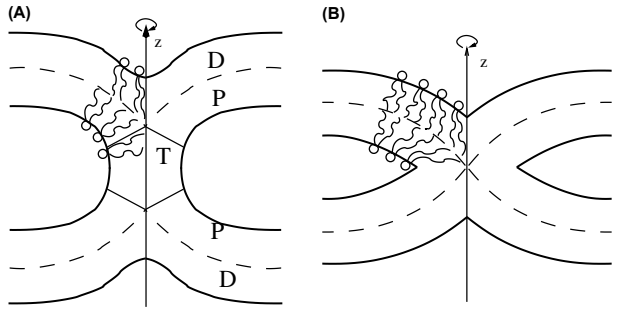

FIGURE 1 Schematic illustration of the fusion stalk model (*A*), and the new suggestion according to Kozlovsky and Kozlov (2002) (*B*). Both structures are rotationally symmetric around the *z* axis and exhibit mirror symmetry with respect to the equatorial plane. The broken lines correspond to the bilayer midplanes. Some lipids are shown schematically. The stalk in *A* consists of three different parts: distal monolayer (D), proximal monolayer (P), and tether (T). The tether contains all those lipids whose hydrocarbon tails point, on average, onto the *z* axis. The stalk in *B* lacks the tether-like connection between the fusing bilayers. Moreover, the profile of the bilayer interfaces exhibits sharp edges and corners.

membranes are directly connected without the formation of a lipidic tether. The key point of their model is the addition of a new internal degree of freedom (that is, another so-called order parameter) into the calculation of the stalk energy. This new degree of freedom is the lipid tilt. It expresses the ability of the hydrocarbon chains to adjust their average orientation. In fact, it is the lipid tilt degree of freedom that allows a fusion stalk to exist without the formation of a void region inside. In the past, the possibility of lipid tilt was frequently recognized (Helfrich, 1973; MacKintosh and Lubensky, 1991; Seifert et al., 1996). Lipid tilt was also investigated in connection with formation of the inverse hexagonal, H_{II}, phase (Hamm and Kozlov, 1998; May and Ben-Shaul, 1999) and lipid-protein interactions (May, 2000; Fournier, 1998, 1999). Kozlovsky and Kozlov (2002) have added the lipid tilt to the ability of the lipid layers to undergo splay deformations. In absence of lipid tilt the splay deformation becomes equivalent to a bending deformation of a lipid layer. Using both these order parameters (splay and tilt), the modified stalk was predicted to have few times smaller energy compared with previous models.

It should be noted that the new stalk structure (that of Fig. 1 *B*) has a property that is absent in previous models: the interface between the hydrocarbon core and the polar environment is no longer smooth at every point. In particular, there is a sharp corner at each side of the stalk, located at the axis of rotational symmetry (the *z*-axis in Fig. 1 *B*). In addition to that, a sharp edge is formed at its waist, where the stalk exhibits mirror symmetry. As discussed by Kozlovsky and Kozlov (2002), the possibility of nonsmooth interfaces arises from the lipid tilt degree of freedom. It allows the formation of a sharp membrane interface without a concomitant divergence of the splay energy.

Let us shortly discuss two other recent approaches to calculate the free energy of fusion stalks. Kuzmin et al. (2001) have suggested a theoretical model that includes, besides bending, tilt of the lipid molecules. The model starts from preformed "nipples" that decrease the local distance of two fusing membranes. It was estimated that this "nipple"-containing bilayers are separated from a fusion stalk structure by an energy barrier of somewhat less than 40 k_BT, in agreement with their estimate (see above). However, creation of the "nipple"-containing bilayers also requires an energy, which in fact is quite high (the authors estimated 200 k_BT). Hence, also the model of Kuzmin et al. (2001) requires an extraordinary high energy to form a stalk out of two apposed, planar bilayers.

In another recent approach, Markin and Albanesi (2002) have postulated a "stress free stalk." The key point of their model is the optimization of the cross-sectional shape of the stalk's neck in terms of its bending energy (rather than being a circular arc, the authors suggest it to be a surface of constant mean curvature). The approach of Markin and Albanesi (2002) indeed leads to very small (in some cases even negative) bending energies of a stalk. However, their model does not solve the principal problem of the large interstitial energy. Indeed, the authors use a reduced interstitial energy and justify this assumption in terms of impurities that fill the interstices and reduce their energy. The lipid tilt degree of freedom is not included in the model of Markin and Albanesi (2002), but the authors discuss its possible influence. They find that, even if using the reduced interstitial energy, a simple tilt deformation of the lipids could give rise to a collapse of the void. This clearly suggests that tilt deformations should be taken into account self-consistently in the calculation of the stalk structure.

In the present work we recalculate the structure and energy of fusion stalks using membrane elasticity theory. One aim of our study is to show that (unlike in the modified structural model suggested by Kozlovsky and Kozlov (2002)) a fusion stalk is likely to contain a tether-like lipidic connection between the two fusing membranes (similarly to that shown in Fig. 1 *A*). To this end, we shall incorporate a tether into our calculations and minimize the stalk free energy with respect to its length. (This implies that the presence of a tether will only be predicted if this is energetically favorable). The main objective of the present study is to clarify the role of the lipid tilt versus the ability of a membrane to form edges (and corners). In particular, we shall argue that the ability of the lipids to tilt is not sufficient to substantially lower the free energy of a fusion stalk. However, it is a necessary condition to allow for the formation of membrane edges. In fact, it is the existence of membrane edges that brings about a remarkable reduction of the stalk's free energy. We shall show this by using exactly the same model to compare lipid stalks with and without the ability to form edges (and corners) included. In the former case, the interfacial region of the stalk can be

nonsmooth, whereas in the latter case it is smooth everywhere. We show that the bare presence of a "smoothness-constraint" leads to a severalfold increase of the stalk's free energy. To this end, we use membrane elasticity theory to optimize the size and shape of the fusion stalk without any further structural assumptions. To summarize, we suggest that, in contrast to most previous calculations of the fusion stalk structure, the interfacial region of a fusion stalk is nonsmooth. Instead, it exhibits edges and corners that crucially influence the stalk's free energy.

THEORY

The fusion stalk structure shown in Fig. 1 *A* is cylindrically symmetric around the *z* axis and exhibits mirror symmetry with respect to the equatorial plane. It consists of three different regions. Two of them, denoted by D and P, form a lipid bilayer with D and P assigned to the distal and proximal monolayer, respectively. The third region, denoted by T, is a tether-like lipidic connection between the two opposite proximal monolayers. The difference between the bilayer part and the tether can clearly be understood in terms of the packing properties of the corresponding lipid molecules. The flexible hydrocarbon chains of the bilayer lipids (that is, those residing in regions D and P) point, on average, onto a two-dimensional surface, namely the midplane of the bilayer (broken lines in Fig. 1 *A*). In contrast, the packing of the lipid chains in the central, tether-like region (T) is similar to that of a cylindrical micelle. Here, the hydrocarbon chains are, on average, directed to a single one-dimensional line. Due to the cylindrical symmetry, this line is straight and corresponds to the *z* axis in Fig. 1 *A*. Consequently, in absence of a tether-like lipidic connection (as is the case in Fig. 1 *B*) all lipids are subject to a bilayer-like packing, and the midplanes of the two apposed bilayers (broken lines in Fig. 1 *B*) touch each other at a single point on the *z* axis.

It is important to realize that the lipids residing within (and close to) a fusion stalk have different physical properties compared with those in a planar, unperturbed bilayer membrane. We refer to these differences as a structural perturbation of the lipids in a fusion stalk. This structural perturbation entails a free energy penalty, *F*, of the stalk. The extent of perturbation is determined by several requirements. First, the lipid chains must be able to fill out the hydrophobic core of the stalk. That is, no void is allowed to form within the entire hydrocarbon chain region. Second, the lipid head groups must protect the hydrocarbon chains from the unfavorable contact with the aqueous environment. Finally, the actual lipid perturbation must minimize the overall free energy, *F*, of the stalk structure.

Free energy of fusion stalk

The hydrophobic core of a fusion stalk (like that shown in Fig. 1 *A*) consists of hydrocarbon chains that are chemically linked to the corresponding polar head groups of the lipids (often through a glycerol backbone, but the exact molecular details do not enter into the present model). The interface between the hydrophobic lipid chains and the polar environment can be specified by a describing surface *A* that we express mathematically by a vector $\mathbf{x}$. (For example, in Fig. 1, *A* and *B*, $\mathbf{x}$ would describe the thick solid lines.) To each position x we can assign a unit vector $\mathbf{n} = \mathbf{n}(\mathbf{x})$, pointing along the average direction of the hydrocarbon chain that originates at $\mathbf{x}$. (Note that we treat all hydrocarbon chains as identical.) Besides by their direction, the lipid tails are also characterized by their (effective) length, b, which results from an average over a sufficiently large number of different chain conformations. Most conveniently, we identify b as the distance between $\mathbf{x}$ and the bilayer midplane (or the z axis if $\mathbf{x}$ belongs to the tether part), measured along $\mathbf{n}(\mathbf{x})$. Using these notations, the structure of the fusion stalk is fully determined by $\mathbf{x}$ and the corresponding directors $\mathbf{b}(\mathbf{x}) = b\,\mathbf{n}(\mathbf{x})$.

Because $\mathbf{x}$ describes a surface, we can associate with each position at $\mathbf{x}$ a unit vector $\mathbf{N}$ that points normal to the surface. Of course, $\mathbf{n}$ and $\mathbf{N}$ need not point into the same direction at any given $\mathbf{x}$. In general, there may be an angle, α, between these two vectors. Mathematically, α is related to the dot product $\mathbf{N} \cdot \mathbf{n} = \cos\alpha$.

The next step is to write down for any given structure of the fusion stalk, as characterized by $\mathbf{b}(\mathbf{x})$, a reasonable expression for the elastic free energy, F. This will finally allow us to find the structure of the fusion stalk such that $F = F[\mathbf{b}(\mathbf{x})]$ adopts a minimum. Within the framework of continuum elasticity, we shall express the free energy, F, of the fusion stalk as an integration over the entire surface A

$$F = \int_A da\, \tilde{f} \tag{1}$$

Assuming sufficiently small local perturbations, we shall use for the elastic free energy density (energy per unit area), $\tilde{f}$, the quadratic expression

$$\tilde{f} = \frac{K}{2} s^2 + \frac{\kappa}{2} (\nabla \cdot \mathbf{n})^2 - \kappa c_0 (\nabla \cdot \mathbf{n}) + \frac{k_t}{2} \alpha^2 \tag{2}$$

The first term in Eq. 2 describes the local compression (or expansion) of the lipid layer; K is the corresponding compression modulus (being equivalent to the lateral compression modulus of a monolayer), and $s = b/b_0 - 1$ is the relative chain dilation with respect to the equilibrium chain length b_0.

The second and third terms in Eq. 2 account for the splay energy of the lipid chains in which κ is the bending stiffness, c_0 is the spontaneous curvature, and $\nabla \cdot \mathbf{n}$ denotes the divergence of the unit vector $\mathbf{n}$. This energy contribution is related to the effective "molecular shape" (Israelachvili, 1992; Evans and Wennerström, 1994) of the lipid mole-

cules. Depending on their chemical structure, and in particular on the bulkiness of the head group versus that of the hydrocarbon chains, lipid molecules may preferentially adopt the shape of a cone, an "inverted" cone, or intermediately that of a cylinder. Deviations of the actual packing geometry of a lipid layer from the preferred one cause an energetic penalty, namely, the splay energy.

The last term in Eq. 2 is the tilt energy of the lipid molecules; k_t is the corresponding tilt modulus. The tilt energy accounts for the angular deviation, α, of the lipid director **b** (or, equivalently, **n**) from the normal direction **N**. We finish this section with five remarks. 1) In their recent approach, Kozlovsky and Kozlov (2002) have used an elastic free energy that is identical to the last three terms of Eq. 2. The only difference of the present approach is, thus, the consideration of the compression/expansion term $Ks^2/2$. Yet, it is exactly this term that is required for a comparison of fusion stalks with and without membrane edges. 2) Generally, there is an additional energetic contribution present in Eq. 2 that accounts for a saddle-splay deformation of the lipid layer. Yet, this term is irrelevant for membrane shape optimization because of the Gauss-Bonnet theorem. Similarly, in the present case, a saddle-splay term would contribute only a constant to the actual minimization of the fusion stalk structure and hence is omitted. 3) The free energy, F, is an excess free energy with respect to a planar and unperturbed lipid layer (for which $s = \alpha = \nabla \cdot \mathbf{n} = 0$). The present work, thus, assumes thermal equilibrium of the lipids residing in the fusion stalk with those far away from it. 4) Generally, the molecular lipid volume remains constant during an elastic deformation of a lipid layer. This conservation would enter the free energy density $\tilde{f}$ in Eq. 2 at higher order than quadratic (unless $c_0 \geqslant 1/b_0$ (May, 2000), but we shall consider sufficiently small spontaneous curvature in the present work). Hence, even though the molecular lipid volume is conserved, it does not enter into the free energy $\tilde{f}$. 5) The expression for the free energy density in Eq. 2 refers to a specific choice of the describing surface, namely the so-called neutral surface. For lipid layers, it is generally reasonable to assume that the neutral surface is located near the interface between the hydrophobic lipid chains and the polar environment (Szleifer et al., 1990).

In the following we shall use the expression for F, defined in Eqs. 1 and 2, to calculate the free energy of a fusion stalk. It is convenient to rewrite the free energy, F, of the entire stalk as a sum of the corresponding free energies of all involved subregions

$$F = F_{bl} + F_T = F_P + F_D + F_T \qquad (3)$$

in which F_{bl}, F_P, F_D, and F_T denote the free energy contributions of the bilayer, proximal monolayer, distal monolayer, and tether, respectively.

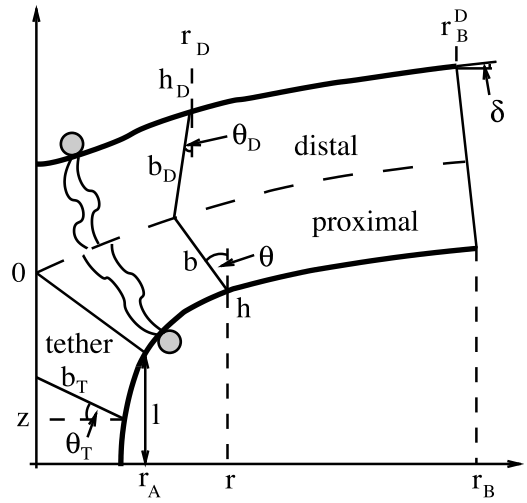

FIGURE 2 Cross-section of a stalk in the r, z-plane; two lipids are shown schematically. Because of the mirror symmetry only the part above the equatorial plane is shown. The structure is rotationally symmetric with respect to the z axis. The thick lines mark the describing surfaces in each of the three regions: distal monolayer, proximal monolayer, and tether. The describing surfaces are located in proximity to the interface between the hydrophobic lipid chains and the polar environment. The broken line between the distal and proximal monolayer marks the midplane of the perturbed bilayer. The proximal monolayer is characterized at its radial coordinate r (with $r_A \leq r \leq r_B$) by the height $h = h(r)$ of the describing surface, by the tilt angle $\theta = \theta(r)$ of the lipid director with respect to the z axis, and by the director length, $b = b(r)$. Similarly, the distal monolayer is characterized at its radial coordinate r_D (with $0 \leq r_D \leq r_B^D$) by the corresponding functions $h_D = h_D(r_D)$, $\theta_D = \theta_D(r_D)$, and $b_D = b_D(r_D)$. Note the angle δ between the bilayer wing and the r axis. Finally, we describe the tether (which has half-length l) with respect to its z coordinate by the tilt angle, $\theta_T = \theta_T(z)$, of the lipid director (measured with respect to the r axis), and by the director length $b_T = b_T(z)$.

Internal degrees of freedom of a fusion stalk

To find the optimal stalk structure and its free energy, F, we shall not rely on any specific assumption on the size and shape of the fusion stalk. Rather, we seek to fully optimize the stalk structure with respect to all relevant degrees of freedom. However, we shall adopt the two following evident structural assumptions. 1) There is an axis of rotational symmetry and a plane of mirror symmetry. This assumption is justified because there is no energetic incentive in our free energy expression that could give rise to a break of symmetry. Conveniently, we use cylindrical coordinates $\{r, \varphi, z\}$ and identify the axis of rotational symmetry with the z axis (see Fig. 1 *A*). 2) The topological structure of the fusion stalk corresponds to that in Fig. 1 *A*. That is, a single lipidic tether connects two perturbed bilayers. Of course, the length of the tether can vary such as to minimize F (for vanishing tether length, the structure in Fig. 1 *B* would be recovered).

Due to the symmetry, we only need to consider, say, the upper one-half of a cross-section of the fusion stalk, which is schematically shown in Fig. 2. The structure of the stalk shown in its cross-section consists of three regions: distal

monolayer, proximal monolayer, and tether. The length of the tether is $2l$; proximal and distal monolayers range from $r_A \le r \le r_B$ and $0 \le r_D \le r_B^D$, respectively (the radial coordinate of the distal monolayer is denoted by r_D).

The shape and structure of each of the three hydrophobic regions is fully characterized by the corresponding function $\mathbf{b}(\mathbf{x})$. As introduced above, $\mathbf{x}$ specifies the shape of the describing surface, *A,* that separates the hydrophobic interior from the polar environment, and $\mathbf{b} = b\,\mathbf{n}$ is the corresponding lipid director (of direction $\mathbf{n}$ and length b). Within the *z, r*-plane, the stalk structure, $\mathbf{b}(\mathbf{x})$, can be represented in each region (proximal monolayer, distal monolayer, and tether) by a number of conveniently chosen functions. In the following, we shall introduce these functions (see also Fig. 2).

The shape vector $\mathbf{x}$ of the proximal monolayer is fully characterized by the local height function, $h = h(r)$, of the describing surface. The corresponding lipid director at position r (with $r_A \le r \le r_B$) is given by the tilt angle with respect to the z axis, $\theta = \theta(r)$, and by the director length, $b = b(r)$.

Analogously to the proximal monolayer, the structure of the distal monolayer, as a function of the radial coordinate r_D (with $0 \le r_D \le r_B^D$), is given by the local height function of the describing surface, $h_D = h_D(r_D)$, by the tilt angle with respect to the z axis, $\theta_D = \theta_D(r_D)$, and by the director length $b_D = b_D(r_D)$.

Whereas the two perturbed monolayers are both described in terms of the radial coordinate, it is more convenient to characterize the tether region with respect to the z axis. One needs two functions, we choose first the tilt angle, $\theta_T = \theta_T(z)$, of the lipid director, measured with respect to the r axis, and second the director length $b_T = b_T(z)$.

Fig. 2 visualizes the geometrical meaning of the functions h, θ, b, h_D, θ_D, b_D, θ_T, and b_T; mathematical definitions of the parameterization, $\mathbf{b}(\mathbf{n})$, in terms of these internal degrees of freedom are given in the Appendix.

So far, the perturbed bilayer (consisting of the proximal and distal monolayer) is characterized by the six functions h, θ, b, h_D, θ_D, and b_D. However, these functions cannot be chosen independently because the two monolayers are structurally coupled. That is, the hydrocarbon chain regions of the respective monolayers have to fit each other without leaving any void. This requirement can easily be put into a simple mathematical condition: For two lipids, whose headgroups are anchored at opposite leaflets of the bilayer, one at position r and the other one at position

$$r_D = r - b \sin\theta + b_D \sin\theta_D \tag{4}$$

the constraint

$$h_D(r_D) = h + b\cos\theta + b_D \cos\theta_D \tag{5}$$

must be fulfilled. Consequently, we refer to Eqs. 4 and 5 as the hydrophobic matching condition. Eq. 5 implies that the perturbed bilayer has not six but only five independent internal degrees of freedom, say $h(r)$, $\theta(r)$, $b(r)$, $\theta_D(r_D)$, and $b_D(r_D)$. Hence, together with the tether region, characterized by $\theta_T(z)$, and $b_T(z)$, we are able to express the structure and free energy of the entire stalk in terms of seven independent functions. In the Appendix, we show how to calculate the separate contributions to the free energy $F = F_P + F_D + F_T$ in terms of the seven independent functions.

Free energy minimization

Generally, the mathematical method of functional minimization provides a convenient way to find the unknown functions, $h(r)$, $\theta(r)$, $b(r)$, $\theta_D(r_D)$, $b_D(r_D)$, $\theta_T(z)$, and $b_T(z)$, such that F adopts a minimum. To this end, seven differential equations (Euler equations) for the seven independent functions can be derived and must be solved with respect to appropriate boundary conditions. However, in the present case this is a formidable task because the Euler equations are nonlinear with respect to the unknown functions. The situation simplifies considerably if we linearize the Euler equations with respect to both an unperturbed membrane (in which $b = b_D = b_0$, $\theta = \theta_D = 0$ and $h = \text{const}$) and a uniform tether (in which $\theta_T = 0$ and $b_T = b_0$). In the present work we use the linearized Euler equations to obtain the conformation of the fusion stalk. This, however, requires us to ensure that the deformation of the stalk is sufficiently small compared with both an unperturbed, planar membrane and a uniform tether. In particular, it must be $\theta(r) \ll \pi/2$ and $\theta_T(z) \ll \pi/2$. On the other hand, at the transition region between the proximal monolayer and the tether (that is at $r = r_A$ and at the corresponding $z_B = z(r_A)$) compactness of the stalk's hydrophobic region can only be achieved if the relation $\theta(r_A) + \theta_T(z_B) = \pi/2$ is fulfilled (see also Fig. 2). Hence, smallness of $\theta(r_A)$ would go at the expanse of $\theta_T(z_B)$ and vice versa. The optimal compromise is where $\theta(r_A) \approx \theta_T(z_B) \approx \pi/4$. In the Results section we show that, indeed, the energetic minimum of the stalk is adopted for the situation where neither $\theta(r_A)$ nor $\theta_T(z_B)$ deviates much from $\pi/4$.

The Euler equations must be solved with respect to certain boundary conditions. Two boundary conditions reflect the compactness of the stalk structure: $\theta_D(r_D = 0) = 0$ and the above-mentioned $\theta(r_A) + \theta_T(z_B) = \pi/2$. Some other boundary conditions can be formulated if one requires the proximal and distal monolayers of the fusion stalk to join an unperturbed bilayer (for which $\tilde{f}$ according to Eq. 2 vanishes everywhere). This implies certain conditions for the lipid directors at positions r_B and r_B^D. If in addition to that we demand $r_B = r_B^D$ then the unperturbed bilayer, joining the stalk, is parallel to the r axis (or, equivalently, to the plane of mirror symmetry). This case is obviously relevant if a stalk is formed starting from two, apposed, parallel bilayers. Yet, this situation need not be the energetically most favorable one. We may, alternatively, allow the bilayer wings to

adjust their angle, δ (see Fig. 2), with respect to the r axis such that F adopts a minimum. The difference of the free energy F for both cases reflects the energetic cost of transforming an energetically optimal stalk into one that connects two parallel membranes. In the Results section we shall consider both cases.

There are two more boundary conditions to be chosen. In fact, these two boundary conditions play a crucial role for the purpose of the present study. One of them specifies the length of the lipid director, b_D, originating at position $r_D = 0$ of the distal monolayer. If the fusion stalk has a smooth interface, then this length must be chosen such that the condition

$$\left(\frac{dh_D(r_D)}{dr_D}\right)_{r_D=0} = 0 \qquad (6)$$

is fulfilled. Alternatively, if the stalk is not required to adopt a smooth interface, $b_D(r_D = 0)$ is allowed to adjust such as to minimize F. In the latter case, the distal monolayer may exhibit a corner at its symmetry axis. The second remaining boundary condition specifies the length, $b(r = r_A)$, of the lipid director at the transition region between the proximal monolayer and the tether. Again, this length may be chosen such as to ensure smoothness of the stalk structure. Alternatively, it can be allowed to adjust to minimize F. In the latter case, the interfacial region of the stalk may exhibit an edge at $r = r_A$. These two different sets of boundary conditions, one ensuring a smooth interface of the stalk and the other one minimizing F at the expansive of forming a nonsmooth interface, are the key point of our present investigation. They allow a direct comparison of the free energies, F, for smooth versus nonsmooth stalks.

RESULTS AND DISCUSSION

We present calculations for the following set of material parameters: $K = 0.35\ k_BT/Å^2$, $\kappa = 6.8\ k_BT$, $c_0 = 0$, $k_t = 0.1\ k_BT/Å^2$, and $b_0 = 14$ Å. The material constants of lipid bilayers obtained by different investigators do often vary, depending on the experimental method and the system (compare Niggemann et al., 1995). Hence, our present choice for K and κ, which follows Evans and Rawicz (1990), is not meant to represent a specific system. Rather, we use it to illustrate the mechanism of how membrane edges reduce the stalk energy. The uncertainty about the correct magnitude is even larger for the tilt modulus, which has not yet been determined experimentally. The value $k_t = 0.1\ k_BT/Å^2$ follows from a simple estimate that directly relates the tilt modulus to the chain stretching rigidity of the lipid chains (May and Ben-Shaul, 1999; Hamm and Kozlov, 1998).

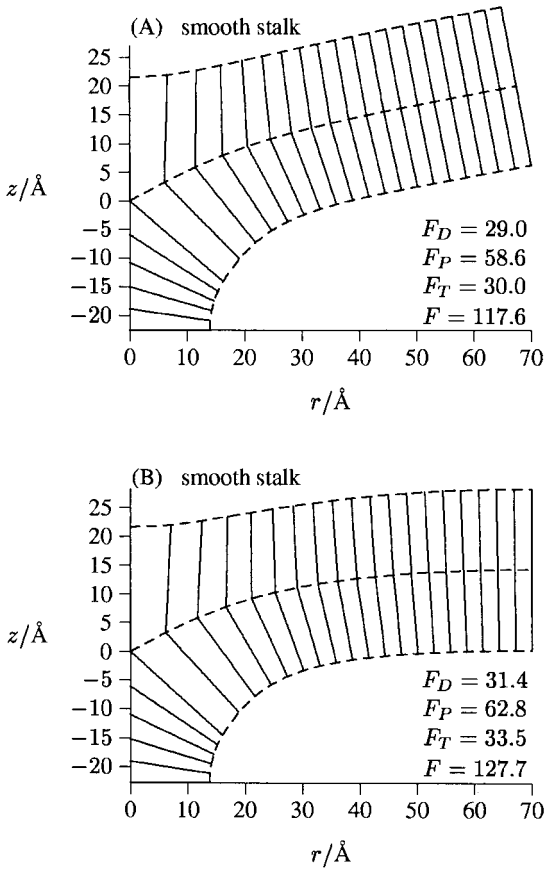

FIGURE 3 Calculated structure of a smooth fusion stalk (with the corresponding free energies, $F = F_P + F_D + F_T$, indicated in units of k_BT) for $K = 0.35\ k_BT/Å^2$, $\kappa = 6.8\ k_BT$, $c_0 = 0$, $k_t = 0.1\ k_BT/Å^2$, and $b_0 = 14$ Å. At $r_B = 70$ Å the bilayer adopts its optimal orientation (*A*) or joins a flat, unperturbed membrane (*B*).

Structure of smooth stalk

We first demand the stalk to have smooth interface everywhere. In this case we must use appropriate boundary conditions for the Euler equations as discussed in the Free Energy Minimization section (the exact boundary conditions are outlined in the Appendix; see Eqs. 19 and 20).

Recall that the bilayer wing of the stalk at r_B either optimizes its orientation (angle δ in Fig. 2) or is forced to be flat ($\delta = 0$). In Fig. 3, *A* and *B*, we present calculations of the corresponding stalk structures for $r_B = 70$ Å. In both cases, the tether half-length l is optimized. The interfacial regions of both structures are smooth everywhere. The corresponding free energies of the stalks are similar but very high. This is in agreement with previous calculations (Siegel, 1993, 1999). The main difference of the present study is that no structural assumptions on the shape and conformation of the stalks is made. We only assume its topological structure and interfacial smoothness everywhere.

The stalk in Fig. 3 *B* is forced to join a flat bilayer (at r_B). Yet, its energy, F, is only marginally higher than the one for

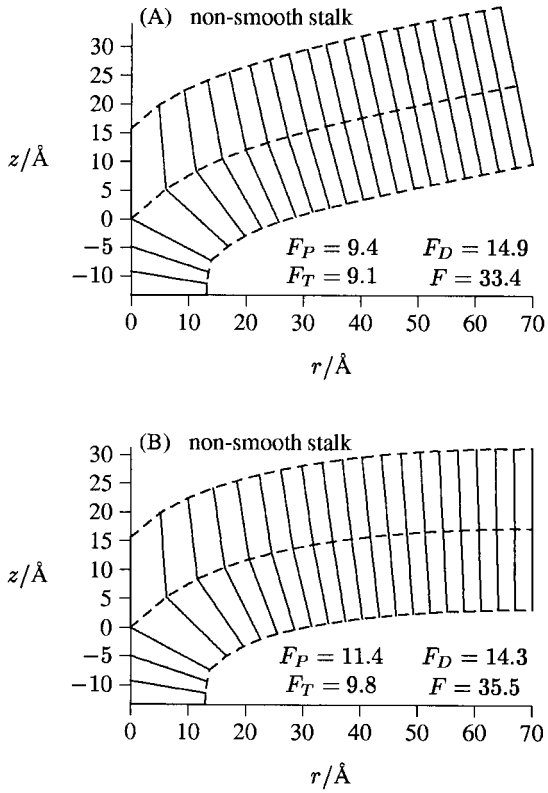

FIGURE 4 Structure of the fusion stalk (with the corresponding free energies, $F = F_P + F_D + F_T$, indicated in units of k_BT) for $K = 0.35$ $k_BT/Å^2$, $\kappa = 6.8$ k_BT, $c_0 = 0$, $k_t = 0.1$ $k_BT/Å^2$, and $b_0 = 14$ Å. At $r_B = 70$ Å, the bilayer adopts its optimal orientation (*A*) or joins a flat, unperturbed membrane (*B*).

optimal bilayer wing orientation displayed in Fig. 3 *A*. This shows that bending of the bilayer at r_B from its optimal orientation into a flat conformation is energetically inexpensive. This allows the conclusion that the stalk energy is relatively insensitive with respect to the membrane-membrane distance of the fusing bilayers. Similarly, we conclude that the stalk energy only weakly depends on the choice of r_B. That is, for any $r_B > 70$ Å, the stalk free energy, F, would be found between the values given in Fig. 3, *A* and *B*. Only a considerably smaller choice of $r_B < r_A + \xi$ would substantially increase F. Here ξ is the decay length of the membrane tilt angle perturbation, which is given by $\xi^{-1} = (2b_0/(\kappa K)^{1/2} + 1/k_t)^{1/2} \times K^{1/2}/2b_0$ (May, 2002). Typically for lipid bilayers (and consistent with our present choice of the material parameters) $\xi \approx 10$ Å. Hence, our present results would be similar for any choice of $r_B \gg r_A + \xi$. Similar considerations also apply for nonsmooth stalks.

Structure of stalk with membrane edges

A stalk structure of much lower free energy forms if sharp membrane edges are allowed to occur. Two corresponding calculations are presented in Fig. 4, *A* and *B*. The stalk in

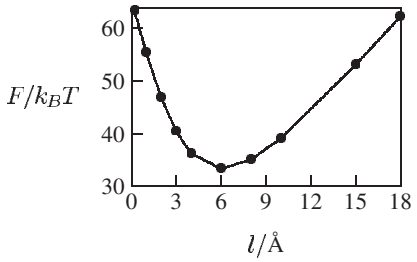

FIGURE 5 Dependence of the stalk free energy on the half-length, l, of the tether. The calculation corresponds to the nonsmooth stalk shown in Fig. 4 *A* with variable l.

Fig. 4 *A* is optimized with respect to the wing orientation of the bilayer (expressed by the angle δ; see Fig. 2); for Fig. 4 *B*, it is $\delta = 0$. The two structures in Fig. 4 differ from the corresponding ones in Fig. 3 only in the choice of those two boundary conditions that specify whether the stalk is forced to be smooth at $r = r_A$ and $r_D = 0$ or not (as discussed in the Free Energy Minimization section).

The stalk structures clearly exhibit edges at the joint between the proximal monolayer and the tether. Moreover, there is a sharp corner located at the intersection between the z axis and the interface of the distal monolayer. This considerably helps the lipid chains to fill up the hydrocarbon region at $r = z = 0$ without causing large lipid layer perturbations. As a consequence, the free energies of the nonsmooth stalks are several times lower compared with the corresponding smooth stalks.

The stalks shown in Fig. 4 have a tether length of $\approx 2l = 12$ Å. Instead of minimizing F with respect to l one can also impose a certain l to the stalk and calculate the corresponding F. We have performed this calculation for the stalk displayed in Fig. 4 *A*; the result is shown in Fig. 5.

The minimum appears at some intermediate l for the following reason. For large l, the length of the tether does not affect the structure of the two perturbed bilayers. Moreover then, the free energy F_T of the cylindrical micelle-like tether is proportional to its length, implying $F \sim l$. The slope of $F(l)$ must be positive because the lipid bilayer is energetically preferred compared with a uniform tether. For small l, the tether nearly vanishes and so does its free energy F_T. Yet, the hydrophobic core of the stalk must be compact, implying $\theta_T(z_B) = 0$ (recall $z_B = z(r = r_A)$). The corresponding lipids have thus a very high tilt angle α, which results in high free energies of the perturbed lipid bilayers. A compromise is offered for intermediate l in which F_T is still small and $\theta_T(z_B)$ can relax to values for which the corresponding lipid tilt deformations are not too high.

Note that $l = 0$ corresponds to the model suggested by Kozlovsky and Kozlov (2002). We shall not attempt to directly compare with their calculated energies for two reasons: First, our approach allows the local lipid chain lengths to adjust and hence contains an additional order parameter. Second, and perhaps more important, our

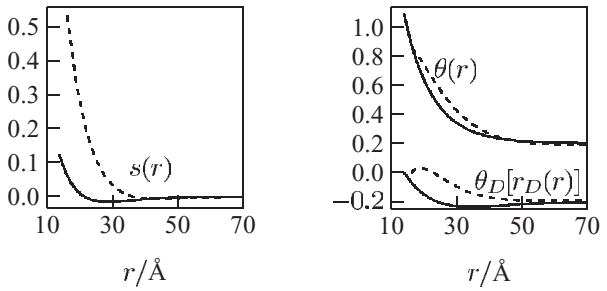

FIGURE 6 Relative chain dilation, $s(r) = b(r)/b_0 - 1$, and tilt angles with respect to the z axis, $\theta(r)$ and $\theta_D[r_D(r)]$, of a smooth (*broken lines*) and nonsmooth (*solid lines*) stalk. The profiles correspond to Figs. 3 *A* and 4 *A*.

method to calculate F assumes small values of θ (this was needed to linearize the Euler equations). Yet, for $\theta(r = r_A) = \pi/2$ as required by $l = 0$ the profile $\theta(r)$ becomes large near r_A, which may induce a substantial overestimation of F. Still, despite our uncertainty regarding $l = 0$, the existence of an energetic minimum for intermediate l is a reliable prediction of the present model. Thus, it is very likely that fusion stalks contain a tether as shown in Fig. 4.

Comparison of smooth with non-smooth stalks

The free energy of the stalks depends strongly on the assumption whether interfacial smoothness is imposed or not. The main structural difference is the degree of chain stretching for those lipids that fill the interstices at $r = z = 0$. This is shown in Fig. 6 for the smooth stalk (broken lines) and nonsmooth stalk (solid lines) displayed in Figs. 3 *A* and 4 *A*, respectively. The left diagram of Fig. 6 shows the relative chain dilation $s(r) = b(r)/b_0 - 1$ for the proximal monolayer. The corresponding relative chain dilation for the distal monolayer, $s_D(r_D) = b_D(r_D)/b_0 - 1$, has the same functional dependence as $s(r)$ (as following from the Euler equations; see Appendix). That is $s_D(r_D) = s(r)$ in which $r_D = r_D(r)$ relates "corresponding" directors according to Eq. 4. Note in particular that $s(r = r_A) = s_D(r_D = 0)$. The right diagram in Fig. 6 displays the tilt angles, $\theta(r)$ and $\theta_D[r_D(r)]$ where, again, the director at r (belonging to the proximal monolayer) and the "corresponding" one at $r_D = r_D(r)$ (belonging to the distal monolayer) point onto the same midplane position as expressed by Eq. 4. The large difference of $s(r)$ at small r between smooth and nonsmooth stalks expresses the different degree of chain stretching, causing substantial differences in the corresponding free energies. What is the reason for the pronounced chain stretching of smooth stalks near the point $z = r = 0$? This stretching results from the packing of the respective lipid chains. On one hand, the lipids must not leave any voids in the hydrophobic interior of the stalk. That means they must (on average) be able to reach the point $z = r = 0$. The lipid packing, on the other hand, becomes very unfavorable if the monolayer's interface is strongly bent towards the point $z = r = 0$. This would create high splay energies for the corresponding lipids. The resulting compromise is an only moderately curved interface, as the cross-sections in Fig. 3 show. Yet, this leads to the large distance between the lipid head groups and the point $z = r = 0$, implying pronounced chain stretching. This situation changes drastically if the constraint of interfacial smoothness is abandoned. Then, the two lipid layers, forming regions P and T (see Fig. 1), can pack separately. An edge is created between regions P and T, but this allows the lipid heads to come close enough to the point $z = r = 0$ to avoid high chain stretching. At the first glance, the presence of an edge might indicate a divergence of the free energy. However, this is not the case as was already pointed out by Kozlovsky and Kozlov (2002). All relevant lipid deformations (those taken into account in Eq. 2) remain finite. Bending of the describing surface itself is not connected with an energetic cost. Hence, there is no reason for an edge (or corner) not to form if this lowers the free energy of the stalk.

TABLE 1 Stalk free energies for smooth ($F = F_{smooth}$) and nonsmooth ($F = F_{nonsmooth}$) membrane interfaces for different values of the tilt modulus k_t

k_t/k_BTÅ^{-2}	0.02	0.1	0.2	0.3
F_{smooth}/k_BT	44.1	117.6	196.7	346.5
$F_{nonsmooth}/k_BT$	17.7	33.4	48.0	60.6

The calculations were performed for the bilayer adopting its optimal orientation at $r_B = 70$ Å.

Dependence on tilt modulus

The present approach is based on the assumption that lipid chains are allowed to tilt with respect to the monolayer's interface. However, the corresponding tilt modulus, k_t, is unknown at present. The value $k_t = 0.1\ k_BT/Å^2$, used to calculate Figs. 3 and 4, results from a simple theoretical estimate (May and Ben-Shaul, 1999; Hamm and Kozlov, 1998). It assumes that upon a uniform tilt of the lipids in a bilayer, the hydrocarbon chains have to stretch to uniformly fill the hydrophobic interior (the thickness of the hydrocarbon core remains unaffected by the tilt deformation). The energy to stretch lipid chains can be roughly related to the stretching modulus K. The resulting prediction $k_t \approx 0.1\ k_BT/Å^2$ is, of course, very crude. Yet, the ability of the lipids to tilt (that is $k_t < \infty$) is the very basis of the present model. With $k_t \to \infty$ membrane edges could not form, and the resulting stalk energies would be very high. It is thus useful to test whether the ability of membrane edges to reduce the energy of stalks is similarly found for other values of k_t. To this end, we compare in Table 1 the free energies F for smooth ($F = F_{smooth}$) and nonsmooth ($F = F_{nonsmooth}$) stalks at different k_t. Clearly, the model is robust with regard to variations in k_t. The nonsmooth stalk always has a much lower energy than its smooth counterpart. We remark that

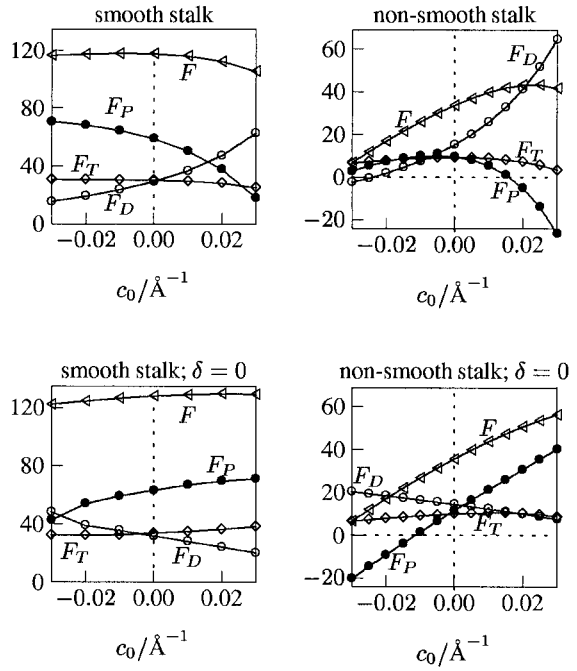

FIGURE 7 Dependence of F and its components (F_D, F_P, and F_T) on the spontaneous curvature, c_0, of the lipid layer (all energies are in units of k_BT) for smooth (*left*) and nonsmooth stalks (*right*). The bilayer is allowed to adopt its optimal wing orientation at $r_B = 70$ Å (*upper diagrams*) or is forced to be flat ($\delta = 0$) at $r_B = 70$ Å (*lower diagrams*). The structures corresponding to $c_0 = 0$ are shown in Figs. 3 and 4.

we cannot perform calculations in the limit $k_t \to \infty$. The reason is the linearization of the Euler equations that we use throughout this work. It only allows us to approximatively calculate the optimal stalk structure. In particular, in the limit $k_t \to \infty$ the tilt angles α will not be predicted to exactly vanish. Therefore, F will diverge for $k_t \to \infty$. If we could exactly minimize F (without linearizing the Euler equations) then we would find a finite value for $F(k_t \to \infty)$. The structures and energies of the smooth and corresponding nonsmooth stalks would then be identical.

Dependence on spontaneous curvature

A quantity that is of considerable experimental interest is the spontaneous curvature, c_o, of the lipid layers. In fact, the stalk free energy is likely to increase with the spontaneous curvature of the lipids. Lipids with highly negative c_0 (like dioleoylphosphatidylethanolamine) are found more fusogenic than those with vanishing or small c_0 (like dioleoylphosphatidylcholine). Lipids with highly positive c_0 (like lysolipids) act as typical fusion inhibitors (Chernomordik et al., 1995b). This behavior is supported only by the model of nonsmooth stalks. To this end, we show in Fig. 7 the dependence of F and its components (F_P, F_D, and F_T) on c_0 for the four stalk structures displayed in Figs. 3 and 4 (these were derived for $c_0 = 0$). The left and right diagrams are calculated for smooth and nonsmooth stalks, respectively. For the two upper diagrams the bilayer wing orientation is allowed to freely adjust at $r_B = 70$ Å; in the two lower diagrams, the bilayers are flat at $r_B = 70$ Å (that is $\delta = 0$). Clearly, for smooth stalks there is essentially no effect of c_0 on F. Contrary to that, nonsmooth stalks considerably lower their free energy if the spontaneous curvature becomes more negative.

Experiments also suggest that addition of fusion-promoting or fusion-inhibiting lipids into either the distal or proximal monolayers have different effects on fusion. When residing in the distal monolayers these lipids affect the formation of the fusion pore. On the other hand, formation of hemifused membranes depends on the presence of these lipids in the proximal monolayers (Chernomordik et al., 1995a). Similar findings were also made for protein-mediated fusion (Chernomordik et al., 1997). With regard to Fig. 7, it is clear that only the right bottom diagram shows a dependence of F_P on c_0 that is consistent with experiment. That is, only the nonsmooth stalk that joins (at r_B) a flat membrane lowers the free energy if the proximal monolayers reduce their spontaneous curvature. Even though the two nonsmooth stalks in Fig. 7 (flat and adjustable bilayer wing orientation at r_B) have very similar energies F, the dependence of their contribution F_P on c_0 differs qualitatively.

The energy, F_T, of the tether is nearly independent of c_0 in all diagrams of Fig. 7. This may appear as a surprise because the tether is structurally similar to a cylindrical micelle. It is well known that common (unperturbed) cylindrical micelles strongly prefer surfactants of positive spontaneous curvature c_0 (Israelachvili, 1992), implying that F_T should be a decreasing function with c_0. Yet, this is not the case in Fig. 7. The reason is that the packing properties of the lipid chains within the tether are actually quite different from those in an unperturbed cylindrical micelle. In fact, when part of a fusion stalk, the tether experiences a large splay deformation in z direction as can be seen in Figs. 3 and 4. It appears that the splay along the z axis is similar in magnitude to that in radial direction but opposite in sign. Hence, the effective total splay, $\nabla \cdot \mathbf{n}$, is small and does not contribute much to the free energy. In light of that, the constancy of $F_T(c_0)$ is no longer a surprise. In a way, this finding is somewhat similar to the suggestion of Markin and Albanesi (2002) that the neck of a fusion stalk is nearly stress free.

CONCLUSIONS

We have directly compared smooth and nonsmooth fusion stalks. The corresponding free energies are remarkably different. It appears that membrane edges dramatically reduce the energy stored in a fusion stalk. Membrane edges become possible through the ability of the lipids to undergo tilt deformations. The corresponding tilt modulus, k_t, is currently not well known. Even though the principal conclu-

sions of the present study remain the same for different choices of k_t, the need for more reliable values of k_t is apparent.

The reduction of the stalk energy through the formation of membrane edges is very similar to the recent findings of Kozlovsky and Kozlov (2002). The main difference is that the present model predicts the existence of a lipidic tether-like connection between the proximal monolayers, whereas this part is absent in the work of Kozlovsky and Kozlov (2002).

APPENDIX

We calculate each of the contribution to the free energy, $F = F_P + F_D + F_T$ (see Eq. 3), derive the corresponding Euler equations, specify the boundary conditions, and comment on the numerical procedure to solve the Euler equations. Note that in all of the following we use cylindrical coordinates $\{r, \varphi, z\}$.

Proximal monolayer

The parameterization of the three functions $h(r)$, $\theta(r)$, and $b(r)$ (see Fig. 2) is given by

$$\mathbf{x} = \{r\cos\phi, r\sin\phi, h(r)\} \tag{7}$$

$$\mathbf{b} = b(r)\{-\cos\phi\sin\theta(r), -\sin\phi\sin\theta(r), \cos\theta(r)\}$$

Instead of $h(r)$ one may equivalently use the local angle, $\psi(r)$, between the height profile and the r axis. The relation between both quantities is $\tan\psi = h'$. (Here the prime denotes the derivative with respect to r).

The free energy F_P can be calculated according to Eq. 1 and Eq. 2 in terms of the three internal degrees of freedom: $\theta = \theta(r)$, $b = b(r)$, and $h = h(r)$. To this end note that $s = s(r) = b/b_0 - 1$, $\alpha = \theta - \psi$, and $\nabla\cdot\mathbf{n} = (r\sin\theta)'/r$. Inserting these expressions into Eq. 2 results in $\tilde{f} = \tilde{f}(s, \theta, \theta', h')$. Because the area element, corresponding to $\mathbf{x}$ in Eq. 7, is $da = 2\pi r\sqrt{1 + h'^2}$ we arrive at

$$F_P = 2\times 2\pi\int_{r_A}^{r_B} dr\, r\sqrt{1 + h'^2}\,\tilde{f}(s, \theta, \theta', h') \tag{8}$$

in which the additional factor of two results from the two proximal monolayers that contribute to the fusion stalk.

Distal monolayer

In Fig. 2, the three internal degrees of freedom of the distal monolayer are denoted by $b_D = b_D(r_D)$, $\theta_D = \theta_D(r_D)$, and $h_D = h_D(r_D)$. Because the distal monolayer behaves energetically equivalent to the proximal monolayer, its free energy, F_D, is calculated analogously to Eq. 8

$$F_D = 2\times 2\pi\int_0^{r_B^D} dr_D r_D\sqrt{1 + h_D'^2}\, f(s_D, \theta_D, \theta_D', -h_D') \tag{9}$$

in which the prime denotes the derivative with respect to r_D. Note that $s_D(r_D) = b_D(r_D)/b_0 - 1$ is the relative chain dilation within the distal monolayer. Also note the negative sign in front of $h_D'(r_D)$, which accounts for the fact that the two monolayers of the bilayer face each other in opposite direction.

In Eqs. 4 and 5, we have introduced the hydrophobic matching condition that expresses the hydrophobic coupling of the two apposed leaflets of a bilayer membrane. This condition will now be integrated into F_D in Eq. 9. To this end, we transform the integration variable in Eq. 9 from r_D to r according to Eq. 4. This means that in the following the function $h_D[r_D(r)] = h_D(r)$ specifies the height profile of the distal monolayer at position $r_D = r_D(r)$, and analogously for $s_D[r_D(r)] = s_D(r)$ and $\theta_D[r_D(r)] = \theta_D(r)$. As a result, F_D in Eq. 9 is written in the form

$$F_D = 4\pi\int_{r_A}^{r_B} dr\, r_D'\, r_D\sqrt{1 + \left(\frac{h_D'}{r_D'}\right)^2}\,\tilde{f}\left(s_D, \theta_D, \frac{\theta_D'}{r_D'}, -\frac{h_D'}{r_D'}\right) \tag{10}$$

where now the prime denotes the derivative with respect to r. Note that $r_D' = r_D'(r)$ and $h_D'(r)$ can be calculated by differentiating Eqs. 4 and 5. Note also that F_D in Eq. 10 accounts for both of the two distal monolayers that contribute to a fusion stalk.

Applying the hydrophobic matching condition (resulting in Eq. 10) allows us to write the free energy, $F_{bl} = F_P + F_D$, of the perturbed bilayer as an integration over the describing surface of the proximal monolayer only

$$F_{bl} = \int_{r_A}^{r_B} dr\,\bar{f}_{bl}(s, s', \theta, \theta', h', s_D, s_D', \theta_D, \theta_D') \tag{11}$$

(with $s' = ds/dr$ etc) in which the free energy density along the r axis, $\bar{f}_{bl}$, is the sum of the integrands of Eqs. 8 and 10. Note that the dependence of $\bar{f}_{bl}$ on s' and s_D' enters through r_D' and h_D'. Eq. 11 is the starting point for deriving the Euler equations of the bilayer region (see Eqs. 14 below).

Tether

Three internal degrees of freedom define the conformation of a single monolayer. (The bilayer has only five degrees of freedom because of the hydrophobic matching condition). The tether is formed by only a single (yet highly bent) monolayer that should, in principle, be characterized by three order parameters: chain dilation, director tilt, and the shape of the midaxis. For a fusion stalk (see Fig. 1 *A*), however, the midaxis of the tether is a straight line because of the angular symmetry. This eliminates one degree of freedom, and we are thus left with only two unknown functions. We use the following parameterization of $\mathbf{b}(\mathbf{x})$

$$\mathbf{x} = \{h_T(z)\cos\phi, h_T(z)\sin\phi, z\} \tag{12}$$

$$\mathbf{b} = h_T(z)\{-\cos\phi, -\sin\phi, \tan\theta_T(z)\}$$

in which $r = h_T(z)$ is the distance of the describing surface from the z axis, and $\theta_T(z)$ is the angle between the director and the r axis.

Let $\psi_T(z)$ denote the angle between the shape, $h_T(z)$, of the tether and the z axis (implying $\tan\psi_T = h_T'$). Note that for the tether region a prime denotes the derivative with respect to z. Based on the definitions in Eqs. 12, we find the tilt angle, $\alpha = \theta_T - \psi_T$, between the director and the normal of the shape profile, and the divergence $\nabla\cdot\mathbf{n} = \cos\theta_T(1/h_T - \theta_T')$. This allows us to calculate the free energy density, $\tilde{f}$, given in Eq. 2 and, hence, the free energy of the tether

$$F_T = 2\times 2\pi\int_{z_A}^{z_B} dz h_T\sqrt{1 + h_T'^2}\,\tilde{f} \tag{13}$$

in which $da = 2\pi h_T\sqrt{1 + h_T'^2}$ is the surface area element, corresponding to $\mathbf{x}$ in Eq. 12; z_A marks the position of the equatorial plane and $z_B = z_A + l$. Note again the prefactor of 2 that accounts for the two (identical) parts of the tether below and above the equatorial plane where the stalk exhibits mirror symmetry.

At this point, we specify the two internal degrees of freedom of the tether region. One is $\theta_T(z)$ and the other $s_T(z) = b_T(z)/b_0 - 1$ in which $b_T(z)$ is the effective lipid chain length. According to Fig. 2 it is $h_T(z) = b_T(z)\cos\theta_T(z)$ that allows us to express the free energy of the tether, $F_T = F_T(s_T, \theta_T)$, fully in terms of $s_T(z)$ and $\theta_T(z)$ (for the corresponding Euler equations see Eq. 15 below).

Euler equations

We consider first the Euler equations that minimize the free energy, F_{bl}, of the perturbed bilayer (see Eq. 11). Because these equations appear as rather complex expressions, we have linearized them with respect to a flat and unperturbed membrane, in which $s(r) = \theta(r) = h'(r) = s_D(r) = \theta_D(r) = 0$. The linearization requires for the resulting stalk conformation $|s(r)| \ll 1$, $|s_D(r)| \ll 1$, $|h'(r)| \ll 1$, $|\theta(r)| \ll \pi/2$, and $|\theta_D(r)| \ll \pi/2$. The resulting Euler equations read

$$
\begin{aligned}
s_D &= s \\
s'' + \frac{s'}{r} &= \frac{K}{b_0^2 k_t}\, s - \frac{1}{2b_0}\left[\theta_D' + \frac{\theta_D}{r} + \theta' + \frac{\theta}{r}\right] \\
\left(\theta_D' + \frac{\theta_D}{r}\right)' &= \frac{k_t}{\kappa}\,(\theta_D + 2b_0 s' + h') + \frac{b_0 c_0}{r^2}\,(\theta - 2\theta_D) \\
\left(\theta' + \frac{\theta}{r}\right)' &= \frac{k_t}{\kappa}\,(\theta - h') + \frac{b_0 c_0}{r^2}\,\theta_D \qquad (14) \\
h'' + \frac{h'}{r} &= -\frac{K}{b_0 k_t}\, s + \theta' + \frac{\theta}{r}
\end{aligned}
$$

Our results for the bilayer conformation are based on numerical solutions of these equations. The bilayer free energy, F_{bl}, is obtained by inserting the solution of Eq. 14 back into Eq. 11.

Next, we calculate the Euler equations that minimize the free energy, F_T, of the tether. Again, we linearize them with respect to a uniform tether, characterized by $s_T(z) = \theta_T(z) = 0$. The linearization is valid in the limit $|s_T(z)| \ll 1$ and $|\theta_T(z)| \ll \pi/2$. The resulting Euler equations are

$$
\begin{aligned}
s_T'' &= \frac{-\kappa + 2(\kappa + b_0^2 K)s_T + 2b_0^2(c_0\kappa + b_0 k_t)\theta_T'}{b_0^2(\kappa - 2b_0 c_0 \kappa + 2b_0^2 k_t)} \\
\theta_T'' &= \left(b_0\frac{k_t}{\kappa} + c_0\right)\left(\frac{\theta_T}{b_0} - s_T'\right) - \frac{\theta_T}{2b_0^2} \qquad (15)
\end{aligned}
$$

It is important to note that the state $s_T(z) = \theta_T(z) = 0$ of the uniform tether does not correspond to its energetically most favorable conformation. This would be obtained by the uniform deformation $\theta_T(z) = 0$ and

$$
s_T(z) = \frac{1}{2\,(1 + b_0^2\, K/\kappa)} \qquad (16)
$$

Obviously, $s_T > 0$, indicating that some chain stretching occurs to compensate for the unfavorable monolayer bending. That is, the hydrocarbon region of an unperturbed tether, which is structurally equivalent to a cylindrical micelle, is somewhat thicker than that of the corresponding unperturbed bilayer. This is in agreement with other models of structural transitions in lipidic systems (Ben-Shaul and Gelbart, 1994).

The solution of the Euler equations, Eqs. 14 and 15, determines the shape and structure of the fusion stalk correctly if the perturbation is sufficiently small. However, smallness of the perturbation does not necessarily apply for a fusion stalk. In this case, the linearized Euler equations predict a shape that may deviate somewhat from the optimal one. The corresponding perturbation free energy, F, will in general be higher than the optimal one. Because in the present work we use the linearized Euler equations, we must refer to F as an upper bound.

Boundary conditions

The first one of Eq. 14 states that corresponding lipid directors (i.e., those whose ends meet at a single point) have the same director length. The four remaining differential equations (Eq. 14) have to be solved with respect to eight appropriate boundary conditions (at r_A and r_B with four boundary conditions at each position).

To specify the four boundary conditions at r_B we shall demand that at this point the two monolayers join an unperturbed bilayer. This implies the three boundary conditions

$$
\theta(r_B) = \psi(r_B), \quad \theta_D(r_B) = -\theta(r_B), \quad s'(r_B) = 0 \qquad (17)
$$

A fourth boundary condition can be specified at r_B, depending on whether the bilayer is forced to be flat ($\delta = 0$ in Fig. 2) or free to choose its optimal spatial orientation (optimal δ in Fig. 2). In the former case $h'(r_B) = 0$ and in the latter $\theta'(r_B) = 0$.

At r_A, another four boundary conditions must be specified. The first, $\theta_D(r_A) = 0$ (recall $\theta_D(r) = \theta_D[r_D(r)]$), ensures compactness of the distal monolayer. The second fixes the z position of the perturbed membrane. Here we require at r_A the midplane to be found at $z = 0$ (see Fig. 2), implying $h(r_A) = -b(r_A)\cos\theta(r_A)$. The two remaining boundary conditions can generally be written as

$$
\theta(r_A) = \theta_0, \quad s(r_A) = s_0 \qquad (18)
$$

They fix the tilt, θ_0, and chain dilation, s_0, of the proximal monolayer at position r_A. Note that because of $s = s_D$ (see the first one of Eq. 14) also the chain dilation of the distal monolayer at the z axis is fixed to be s_0. The question arises how θ_0 and s_0 should be chosen. This question directly concerns the smoothness of the stalk's interface. We consider the two possibilities of a smooth and a nonsmooth stalk. 1) For a smooth stalk, s_0 must be chosen such that the interfacial profile of the distal monolayer does not exhibit a corner at the z axis. This gives rise to Eq. 6, or, equivalently, to

$$
\left(\frac{h_D'}{r_D'}\right)_{r=r_A} = 0 \qquad (19)
$$

in which $h_D' = h_D'(r)$ and $r_D' = r_D'(r)$ can be calculated using the hydrophobic matching condition given in Eqs. 4 and 5. Similarly, if the interfacial profile of the proximal monolayer is required to be smooth then also θ_0 must be determined such that the relation

$$
\psi(r_A) + \psi_T(z_B) = \frac{\pi}{2} \qquad (20)
$$

is fulfilled. Hence, for a smooth stalk Eqs. 19 and 20 replace Eq. 18. 2) If interfacial smoothness is not required then the stalk may adjust s_0 and θ_0 such as to minimize its overall free energy, F.

We proceed with a comment on the choice of r_A, which is given by $r_A = b(r_A)\sin\theta(r_A)$. Obviously, r_A itself depends on the functions $s(r)$ and $\theta(r)$, which can be determined only after first specifying the region $r_A \ldots r_B$. However, in our numerical solutions of the Euler equations, we have designed a simple iteration scheme to self-consistently calculate r_A such that the relation $r_A = b(r_A)\sin\theta(r_A)$ is fulfilled.

Consider now the boundary conditions for the tether. At the equatorial plane ($z = z_A$ denotes this position) symmetry requires $s_T'(z_A) = \theta_T(z_A) = 0$. At $z_B = z_A + l$ the tether must match the perturbed bilayer, implying $b(r_A) = b_T(z_B)$ and $\theta_T(z_B) = \pi/2 - \theta_0$ (recall that θ_0 is defined in Eq. 18). In fact, the last two boundary conditions define a compact transition region

between the bilayer and tether. If beyond compactness, we also demand smoothness of the interfacial region, then (as already mentioned above) θ_0 must be adjusted until Eq. 20 is fulfilled.

Numerical procedure to optimize stalk structure

The numerical calculations of the stalk structure were performed according to the following procedure. For any given s_0 and θ_0 one can solve the Euler equations for the bilayer region, Eq. 14, within $r_A \leq r \leq r_B$, and the Euler equations for the tether, Eq. 15, in a region of length l.

Whereas r_B is fixed at some given value (we use $r_B = 70$ Å) we determine r_A self-consistently such that the condition $r_A = b_0(1 + s_0)\sin\theta_0$ is fulfilled. This is achieved by iteratively solving Eq. 14 and updating r_A in each iteration step. We are thus able to calculate the stalk structure and its corresponding energy $F = F(s_0, \theta_0, l)$ as a function of s_0, θ_0, and l. For nonsmooth stalks there is no further structural constraint, implying that $F = F(s_0, \theta_0, l)$ must adopt its minimum. (Alternatively, we can also minimize F with respect to only s_0 and θ_0 and observe the dependence of F on the half-length, l, of the tether).

For smooth stalks, the situation is different. Here, s_0 and θ_0 must be chosen such that Eqs. 19 and 20 are fulfilled. This can be done for any choice of l. Finally, the stalk energy F is minimized with respect to l.

I would like to thank Misha Kozlov for illuminating discussions and for sending a manuscript prior to publication. This work is supported by Thüringer Ministerium für Wissenschaft, Forschung und Kunst.

REFERENCES

Basánez, G., F. M. Goni, and A. Alonso. 1998. Effect of single chain lipids on phospholipase C-promoted vesicle fusion: a test for the stalk hypothesis of membrane fusion. *Biochemistry.* 37:3901–3908.

Basánez, G., M. B. Ruiz-Arguello, A. Alonso, F. M. Goni, G. Karlsson, and K. Edwards. 1997. Morphological changes induced by phospholipase C and by sphingo myelinase on large unilamellar vesicles: a cryo-transmission electron microscopy study of liposome fusion. *Biophys. J.* 72:2630–2637.

Ben-Shaul, A., and W. M. Gelbart. 1994. Statistical thermodynamics of amphiphile self-assembly: structure and phase transitions in micellar solutions. W. M. Gelbart, A. Ben-Shaul, and D. Roux, editors. *In Micelles, Membranes, Microemulsions, and Monolayers,* 1st ed, section 1. Springer, New York. 359–402

Burger, K. N. J. 2000. Greasing membrane fusion and fission machineries. *Traffic.* 1:605–613.

Chanturiya, A., L. V. Chernomordik, and J. Zimmerberg. 1997. Flickering fusion pores comparable with initial exocytotic pores occur in protein-free phospholipid bilayers. *Proc. Natl. Acad. Sci. U.S.A.* 94: 14423–14428.

Chernomordik, L., A. Chanturiya, J. Green, and J. Zimmerberg. 1995a. The hemifusion intermediate and its conversion to complete fusion: regulation by membrane composition. *Biophys. J.* 69:922–929.

Chernomordik, L. V., M. M. Kozlov, and J. Zimmerberg. 1995b. Lipid in biological membrane fusion. *J. Membr. Biol.* 146:1–14.

Chernomordik, L. V., E. Leikina, V. Frolov, P. Bronk, and J. Zimmerberg. 1997. An early stage of membrane fusion mediated by the low pH cconformation of influenza haemagglutinin depends upon membrane lipids. *J. Cell. Biol.* 136:81–93.

Chernomordik, L. V., and J. Zimmerberg. 1995. Bending membranes to the task: structural intermediates in bilayer fusion. *Curr. Opin. Struct. Biol.* 5:541–547.

Epand, R. M. 2000. Membrane fusion. *Biosci. Rep.* 20:435–441.

Evans, D. F., and H. Wennerström. 1994. *The Colloidal Domain, Where Physics, Chemistry, and Biology Meet,* 2nd ed. VCH Publishers, New York.

Evans, E., and W. Rawiez. 1990. Entropy-driven tension and bending elasticity in condensed-fluid membranes. *Phys. Rev. Lett.* 64: 2094–2097.

Fournier, J. B. 1998. Coupling between membrane tilt-difference and dilation: a new "ripple" instability and multiple crystalline inclusions phases. *Europhys. Lett.* 43:725–730.

Fournier, J. B. 1999. Microscopic membrane elasticity and interactions among membrane inclusions: interplay between the shape, dilation, tilt and tilt difference modes. *Eur. Phys. J. E.* 11:261–272.

Gaudin, Y. 2000. Rabies virus-induced membrane fusion pathway. *J. Cell. Biol.* 150:601–612.

Hamm, M., and M. M. Kozlov. 1998. Tilt model of inverted amphiphilic mesophases. *Eur. Phys. J. B.* 6:519–528.

Helfrich, W. 1973. Elastic properties of lipid bilayers: theory and possible experiments. *Z. Naturforsch.* 28:693–703.

Israelachvili, J. N. 1992. *Intermolecular and Surface Forces.* Academic Press, New York.

Jahn, R., and T. C. Südhof. 1999. Membran fusion and exocytosis. *Annu. Rev. Biochem.* 68:863–911.

Kozlov, M. M., and V. S. Markin. 1983. Possible mechanism of membrane fusion. *Biofizika.* 28:242–247.

Kozlovsky, Y., and M. M. Kozlov. 2002. Stalk model of membrane fusion: solution of energy crisis. *Biophys. J.* 82:882–895.

Kuzmin, P. I., J., Zimmerberg, Y. A. Chizmadzhec, and F. S. Cohen. 2001. A quantitative model for membrane fusion based on low-energy intermediates. *Proc. Natl. Acad. Sci. U.S.A.* 98:7235–7240.

Lee, L., and B. R. Lentz. 1997. Evolution of lipidic structures during model membrane fusion and the relation of this process to cell. *Biochemistry.* 36:6251–6259.

Lentz, B. R., V. Malinin, and M. E. Haque. 2000. Protein machines and lipid assemblies: current views of cell membrane fusion. *Curr. Opin. Struct. Biol.* 10:607–615.

MacKintosh, F. C., and T. C. Lubensky. 1991. Orientational order, topology, and vesicle shapes. *Phys. Rev. Lett.* 67:1169–1172.

Markin, V. S., and J. P. Albanesi. 2002. Membrane fusion: stalk model revisited. *Biophys. J.* 82:693–712.

May, S. 2000. Protein-induced bilayer deformations: the lipid tilt degree of freedom. *Eur. Biophys. J.* 29:17–28.

May, S. 2002. Membrane perturbations induced by integral proteins: role of conformational restrictions of the lipid chains. Langmuir. 18: 6356–6364.

May, S., and A. Ben-Shaul. 1999. Molecular theory of lipid-protein interaction and the L_α-H_{II} transition. *Biophys. J.* 76:751–767.

Müller, M., K. Katsov, and M. Schick. 2002. New mechanism of membrane fusion. *J. Chem. Phys.* 116:2342–2345.

Niggemann, G., M. Kummrow, and W. Helfrich. 1995. The bending rigidity of phosphatidylcholine bilayers: dependences on experimental method, sample cell sealing and temperature. *J. Phys. II France.* 5:413–425.

Noguchi, H., and M. Takasu. 2001. Fusion pathways of vesicles: a Brownian dynamics simulation. *J. Chem. Phys.* 115:9547–9551.

Seifert, U., J. Shillcock, and P. Nelson. 1996. Role of bilayer tilt difference in equilibrium membrane shapes. *Phys. Rev. Lett.* 77:5237–5240.

Siegel, D. P. 1993. Energetics of intermediates in membrane fusion: comparison of stalk and inverted micellar mechanism. *Biophys. J.* 65: 2124–2140.

Siegel, D. P. 1999. The modified stalk mechanism of lamellar/inverted phase transitions and its implication for membrane fusion. *Biophys. J.* 76:291–313.

Szleifer, I., D. Kramer, A. Ben-Shaul, W. M. Gelbart, and S. A. Safran. 1990. Molecular theory of curvature elasticity in surfactant films. *J. Chem. Phys.* 92:6800–6817.

Zimmerberg, J., S. S. Vogel, and L. V. Chernomordik. 1993. Mechanisms of membrane fusion. *Annu. Rev. Biophys. Biomol. Struct.* 22:433–466.